Experimental report

01/02/2024

Proposal: **DIR-273** **Council:** 10/2022

Title: Reflection of gravitational UCN quantum states in silicon channels

Research area: Methods and instrumentation

This proposal is a new proposal

Main proposer: **Rene SEDMIK**

Experimental team: Rene SEDMIK
Elias PESCOLLER
Naoto MUTO

Local contacts: Tobias JENKE
Hanno FILTER

Samples:

Instrument	Requested days	Allocated days	From	To
PF2 EDM	23	23	10/05/2023	02/06/2023

Abstract:

This proposal aims to test the distortion-free reflection of UCN quantum states off of vertical etched walls on a silicon wafer, which is a required technology for the next generation experiment of the qBounce collaboration using a storage ring. The latter experiment will study stored gravitationally bound quantum states of UCN, and is likely to improve the accuracy of gravity tests of neutrons by up to 4 orders of magnitude

Report

Reflection of gravitational UCN quantum states in silicon channels, DIR-273

prepared by René Sedmik

Scope

This document gives a brief report of the measurements performed during beamtime DIR-273 and the lessons learned. The file amends the experimental report on 3-14-422 and DIR-245.
The purpose of the proposed measurements was to demonstrate the disturbance-free reflection of gravitational UCN quantum states off of vertical silicon walls and channels.

Measurements

Setup

We used the same basic setup for measurements, as was used during 3-14-22 and DIR-245, resembling the one used for quantum bouncing ball measurements in 2009 [1]. As this setup was described in detail in the previous report on DIR-245, we do not discuss the basic setup here. We performed measurements in four different configurations. First, after the absorber (state selector), we placed a counter detector to determine the basic rate and operation of the absorber (Zero configuration). Subsequently, the counter detector was replaced by a position-sensitive emulsion detector [5] (configuration A) to determine the state distribution resulting from the combination of velocity selector and absorber. In later stages, the position-sensitve detector was shifted further away from the reactor and a flat glass mirror of 50 mm length was inserted after the absorber, serving as a reference without channels (config. B1). In order to measure the beam divergence, a ZrO2 block was placed onto the glass mirror (config. B2). Eventually, a silicon wafer with etched channels was mounted on top of the flat mirror (config. C).

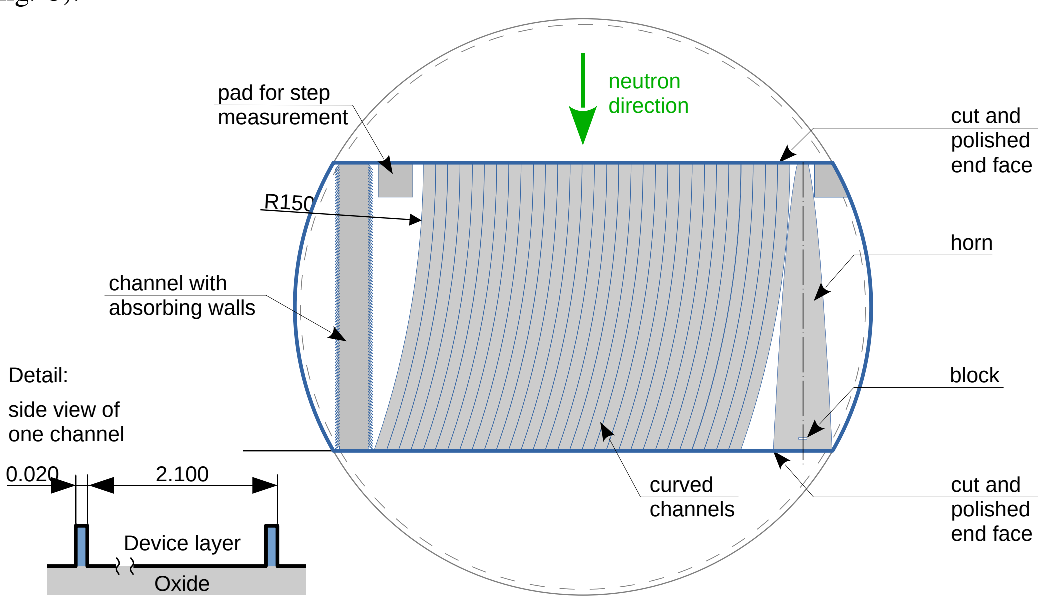

Figure 1: Overview of the different channels on the silicon wafer.

In order to measure and remove any steps between the mirror of the state selector (region I) and the second mirror (or wafer), an absolute distance fiber-based laser interferometer with active PID feedback was used that measured the distance between the mirror (or wafer) surface and a gantry bridging over the setup. The fibers were

continuously moved back and forth between the two regions using a translator stage, resulting in a RMS step of 53.7±6.8 nm during all measurements.
The channels investigated during this beamtime (see Figure 1) were etched into a 100 µm thick <110> wafer bonded to an optically flat glass wafer, using a Bosch process. In order to increase UCN reflectivity, the etched wafer was coated with Ni/Mo (stochiometric ratio 85:15wt%, grey areas).
With respect to previous measurements during 3-14-422, we implemented several changes. SOI wafers were replaced by 2.5 mm thick glass wafers that where optically polished and checked for planarity prior to bonding to a Si wafer and etching. This resulted in a bow/warp smaller than 1 µm over the surface area used for the channels. Front and back edges of the glass wafer were etched with HF with a small step (10 µm) prior to cutting the wafer with a diamond saw, leading to reduced edge deformations and chipping, as observed in 3-14-422. The TiW coating was replaced by NiMo. Sputter coating was performed in a cleanroom directly after etching. No glue was used to mount the wafer to avoid mechanical stress. The glass wafer was held on our mirror by Casimir and adhesion forces instead. Finally, the wafer surface was exposed only for a few minutes to air at NivD during the mounting process and no cleaning liquids were used on the wafer.

Before the start of the measurements, several days of debugging were necessary, as the epoxy seal of the qBouncino chamber used in this experiment needed to be replaced in several spots, as cracks created a massive vacuum leak, and pumping times were increased due to a too small vacuum pump (Edwards XDS10, only later replaced by Edwards XDS35). These problems could be avoided by vacuum tests prior to the beamtime.

Results

Velocity distribution

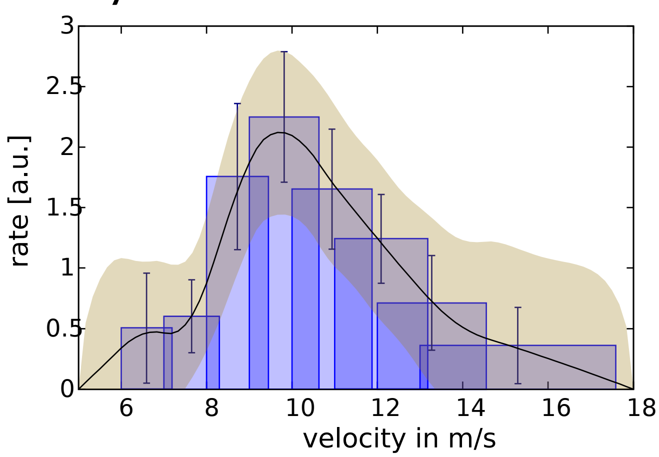

Figure 2: Histogram of the recorded rates (blue bars) for different velocities, fitted curve (black line) with its one sigma probability band (brown band). Graph by E. Pescoller.

Table 1: Measured rates for various velocity settings.

v_{min} [m/s]	v_{min} [m/s]	rate [mcps]	background [mcps]
6	*7.19*	*12.84±1.43*	*0.60±0.54*
7	*8.3*	*38.52±2.65*	*3.67±0.88*
8	*9.44*	*33.47±2.49*	*2.71±0.80*
9	*10.63*	*34.95±2.78*	*3.10±0.93*
10	*11.88*	*17.12±1.14*	*0.78±0.39*
11	*13.18*	*27.19±2.37*	*2.54±0.87*
12	*14.55*	*28.35±3.13*	*1.82±1.00*
13	*17.58*	*10.58±1.26*	*1.66±1.44*
6	*17.58*	*123.48±2.65*	*14.57±0.84*

We measured the velocity distribution after the absorber by means of rate measurements with different settings for the velocity-selecting aperture mechanism. The resulting distribution is shown in Figure 2, while the corresponding numeric results are given in Table 1. Note that the "background" rates refer to residual neutrons arriving at the detector when the PF2 switcher was not in EDM position but shutters were still open. A background measurement representative for the real detector background (2.15±0.09 mcps) was performed during emulsion detector measurements where the detector was placed in the back of the chamber and facing the back-side wall. The freshly clamped absorber produced a rate of 124.8±2.6 mcps (ID 1.001) at a "background" of 16.7±0.8 mcps.

Angular distribution (beam divergence)

In order to derive the beam divergence, we performed Monte Carlo simulations to obtain test data that was then compared with the recorded lateral neutron distribution using a Kolmogorov-Smirnov test. The free parameters in this test were the lateral offset x_B of the detector with respect to the block and the width θ of

θ [°]

an assumed normal distribution of angles with zero mean. The exit coordinates of neutrons at the absorber exit were chosen from a homogeneous distribution, while the forward velocity was chosen from the measured velocity distribution. Figure 3 shows the results of the resulting probability distribution. From these data, we deduce a most probable width of the beam divergence of ~5°. While this is inconsistent with respective values from qBounce (21°), it is consistent with the angle derived from the half width of the absorber exit (47 mm) and the distance from the exit of the beam tube (409 mm), 6.6°.

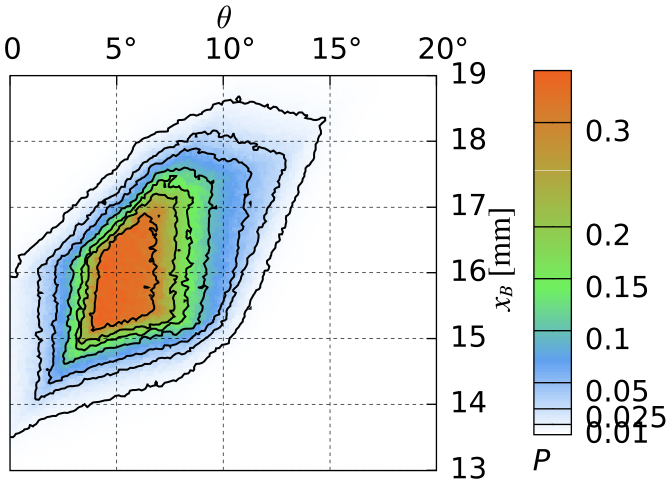

Figure 3: Distribution of the probability P for rejecting the Null hypothesis resulting from a Kolmogorov-Smirnov evaluation using Monte-Carlo simulations of the expected neutron distribution on the detector for variable lateral offset of the detector x_B and width of the angular distribution θ. The 95% Significance interval is θ2[2°,11°] due to rather low statistics of N=660 neutrons in the region shadowed by the block. Graph by E. Pescoller.

Emulsion detector evaluations

All exposed position-sensitive detectors were analyzed by our collaborators around T. Ariga, M. Hino, K. Hirota, G. Ichikawa, S. Kawasaki, M. Kitaguchi, K. Mishima, N. Naganawa, M. Nakamura, O. Sato, Y. Seki, H.M. Shimizu, and A. Umemoto, as described in Ref. [5]. Configuration A gave the state distribution shown in Figure 4a. The block measurement of the beam divergence had quite low statistics, which led to large uncertainties in the fitted divergence angle. Eventually, the results for configuration C (wafer test) showed a large vertical scattering of the neutrons, which was unexpected. Potential causes of these effects were extensively investigated post-beamtime with the result that surface corrugations from etching and problems with the sputter-coating process were most likely responsible for the failure of the test. While these problems have to be solved before a new attempt with neutrons can be made, the emulsion detectors performed perfectly during all tests.

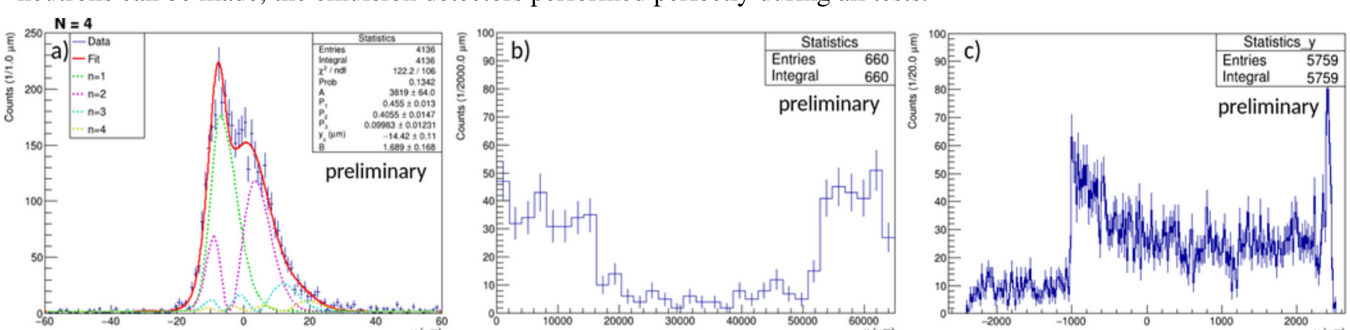

Figure 4: Histograms of detected neutrons. a) Vertical histogram for configuration A used to determine the state distribution. Fit results with reduced χ^2=1.22 for the probabilities P_i of states 1,2,3 are given in the insert. The distribution is virtually identical for configuration B1 (not shown) b) Horizontal histogram for configuration B2 used to extract the angular divergence angle. c) Vertical histogram for configuration C. Graphs by N. Muto.

References

[1] T. Jenke *et al.*, Nucl. Instrum. Methods Phys. Res. **611**, 318 (2009).

[2] T. Jenke *et al.*, Nat. Phys. **7**, 468 (2011).

[3] G. Cronenberg *et al.*, Nat. Phys. **14**, 1022 (2018).

[4] R. I. P. Sedmik *et al.*, EPJ Web Conf. **219**, 05004 (2019).

[5] N. Muto *et al.*, J. Inst. **17**, P07014 (2022).

[6] H. Suzuki *et al.*, CIRP Annals **66**, 93 (2017).